Solar neutrino zenith angle distribution and uncertainty in Earth's matter density

Lian-You Shan and Xin-Min Zhang
Institute of High Energy Physics, Chinese Academy of Science, P.O. Box 918, Beijing 100039, People's Republic of China
(Received 6 January 2002; published 24 June 2002)

We estimate in this paper the errors in the zenith angle distribution for the charged current events of the solar neutrinos caused by the uncertainty of Earth's electron density. In the model of the Preliminary Reference Earth Model with a 5% uncertainty in the Earth's electron density we numerically calculate the corrections to the correlation between $[N]_5/[N]_2$ and $[N]_2/[N]_3$, and find the errors notable.

DOI: 10.1103/PhysRevD.65.113011 PACS number(s): 13.15.+g, 14.60.Lm, 14.60.Pq, 26.65.+t

Forthcoming results from SNO [1] include a measurement of the day-night asymmetry (A_{DN}) [2–5]. This measurement is crucial to confirming the matter conversion solution to the solar neutrino problem. The analysis on the zenith angle distribution of the events during the night may provide some insight into distinguishing the various Mikheyev-Smirnov-Wolfenstein (MSW) solutions, i.e., large mixing angle (LMA), low mass, low probability (LOW), and small mixing angle (SMA) [6]. In the calculation of the regenerated ν_e flux, the electron density of Earth's matter with which the neutrinos interact is a critical quantity. The uncertainty in Earth's matter density and chemical components can be a major cause of error in A_{DN} and the zenith angle distribution. So it will be interesting to estimate these errors. Furthermore, since the experimental value of A_{DN} is around ~ 0.047 [2] and the theoretical expectations on the zenith angle distributions are small in magnitude [6], it is necessary to perform a quantitative estimation on these errors.

In this paper we follow the procedure outlined in [7] and study the uncertainty in Earth's matter density, then investigate its implications on the predictions of A_{DN} and the zenith angle distributions. We quantify the uncertainties of Earth's matter in terms of two parameters: one is $\delta N_e/N_e$, the variation in magnitude of the density which generally is expected to be around a few percent; the second one is δx which specifies the limitation on the spatial dimension by geophysics experiments and inverting calculations used in the fit of Earth's density models. In general the scale δx is not much larger than the neutrino oscillation length, e.g., in the case with the parameters of the favored LMA solution, so its effect might arise beyond the linear order. We will show in this paper that this effect causes a sizable error in the zenith angle distributions.

To begin with we consider a two-neutrino mixing model for simplicity. As discussed in [4,8] the neutrino can be treated as a incoherent mixture of two mass eigenstates. In the daytime the survival probability for ν_e is given by

$$P^D = P_1 \cos^2\theta + (1-P_1)\sin^2\theta, \qquad (1)$$

where the mixing angle is defined through,

$$\nu_1 = \cos\theta\nu_e - \sin\theta\nu_\mu, \quad \nu_2 = \sin\theta\nu_e + \cos\theta\nu_\mu, \qquad (2)$$

and P_1 is the probability of the $\nu_e \to \nu_1$ conversion inside the Sun [9,6]. During the night-time, the presence of Earth's matter leads to a zenith angle dependent regeneration of the ν_e,

$$P^N = P_1 + (1-2P_1)P_{2e} = P^D - 2Xf_{reg}, \qquad (3)$$

where P_{2e} is the probability of the $\nu_2 \to \nu_e$ conversion inside the Earth, $X = P_1 - 1/2$. And

$$f_{reg}(\theta_z) \equiv P_{2e}(\text{Earth's matter}) - P_{2e}(\text{vacuum}), \qquad (4)$$

is the regeneration factor which vanishes in the absence of Earth's matter effect. Defining $\overline{f_{reg}}$ as the regeneration factor integrated over the zenith angle, one has the day-night asymmetry,

$$A_{DN} \equiv \frac{P^N - P^D}{\frac{1}{2}(P^N + P^D)} = \frac{-2X\overline{f_{reg}}}{0.5 + (\cos 2\theta - \overline{f_{reg}})X}. \qquad (5)$$

The matter effects have entered the day-night asymmetry through f_{reg}. Formally,

$$P_{2e}(E_\nu, \theta_z) = \bigg| \cos\theta \lfloor \mathcal{T}\exp\lfloor -i\int_0^{D\cos\theta_z} H[N_e^{\theta_z}(x)]dx \rfloor\rfloor_{ee} + \sin\theta \lfloor \mathcal{T}\exp\lfloor -i\int_0^{D\cos\theta_z} H[N_e^{\theta_z}(x)]dx \rfloor\rfloor_{e\mu} \bigg|^2, \qquad (6)$$

where $D = 12742$ is the diameter of Earth in kilometers and $H[N_e^{\theta_z}(x)]$ is the effective Hamiltonian for the given trajectory with zenith angle θ_z,

$$H[N_e^{\theta_z}(x)] = \frac{\Delta m^2}{4E_\nu}\begin{pmatrix} 2\sin^2\theta & \sin 2\theta \\ \sin 2\theta & 2\cos^2\theta \end{pmatrix} + \begin{pmatrix} \sqrt{2}G_F N_e^{\theta_z}(x) & 0 \\ 0 & 0 \end{pmatrix}. \qquad (7)$$

In Eq. (7), $N_e^{\theta_z}(x)$ is Earth's electron density (EED) along the trajectory of the zenith angle θ_z. If the density is known, the regeneration factor $f_{reg} = P_{2e} - \sin^2\theta$ can be calculated accurately. As an example we take the Preliminary Reference Earth Model (PREM) [10] and plot in Fig. 1(a) the regenera-

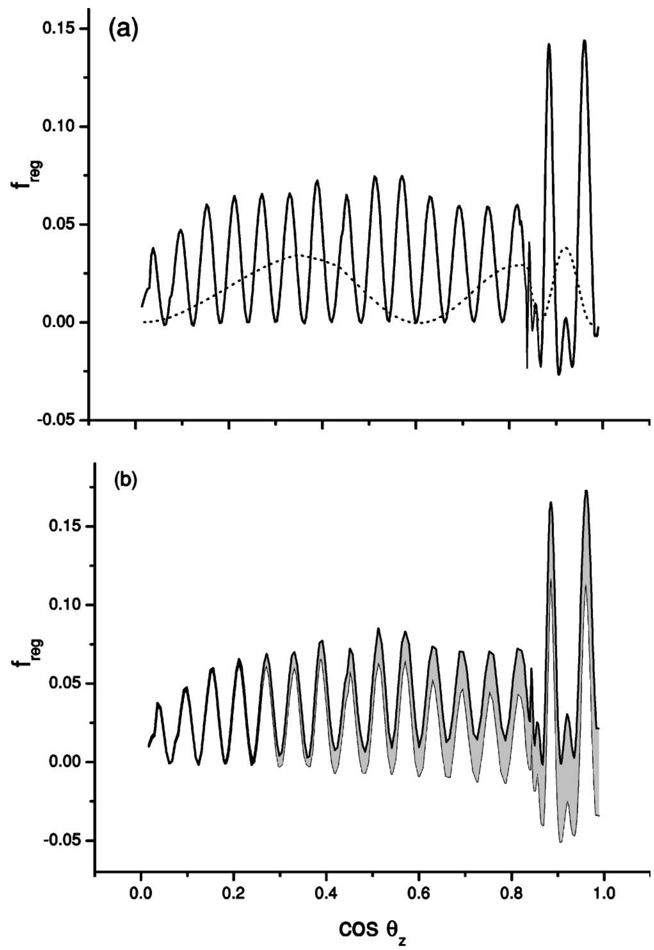

FIG. 1. Plot of the regeneration factor vs the zenith angles for neutrino energy at 11 MeV. Earth's matter model of the PREM and the neutrino oscillation parameters in Eq. (8) have been used. (a) The solid line is for the LMA while the dotted line is for the LOW. (b) The error bars correspond to the corrections due to the 5% uncertainty in the matter density (the PREM). The fluctuation in the LOW case is smaller than the LMA case, so we have not shown them explicitly in this figure.

tion factor as a function of the zenith angle. In the numerical calculation we take the neutrino energy to be 11 MeV and the oscillation parameters to be [11]

$$\text{LMA:}\quad \Delta m_{12}=3.7\times10^{-5},\quad \tan^2\theta=0.37,$$

$$\text{LOW:}\quad \Delta m_{12}=1.0\times10^{-7},\quad \tan^2\theta=0.67. \qquad (8)$$

One can see from this figure that the regeneration factors oscillate periodically with certain lengths. And different oscillation lengths correspond to different MSW solutions.

Given the parameters in Eq. (8) and the standard solar density [12], we follow [6,9] and obtain numerically that $\cos 2\theta_S \approx -1$ and $P_c \approx 0$, which can be used to get the $\nu_e \to \nu_1$ conversion in the Sun. Fluctuations in the solar density will affect P_1, and consequently also influence the MSW solutions [13]. In that situation a variance of P^D has been

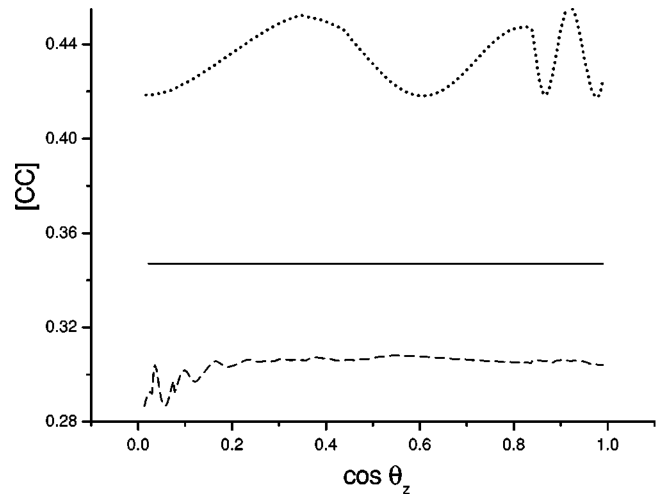

FIG. 2. Charged current event rates vs the zenith angles. The dotted line is for the LOW and the dashed line for the LMA. The solid straight line is the data of the SNO observation.

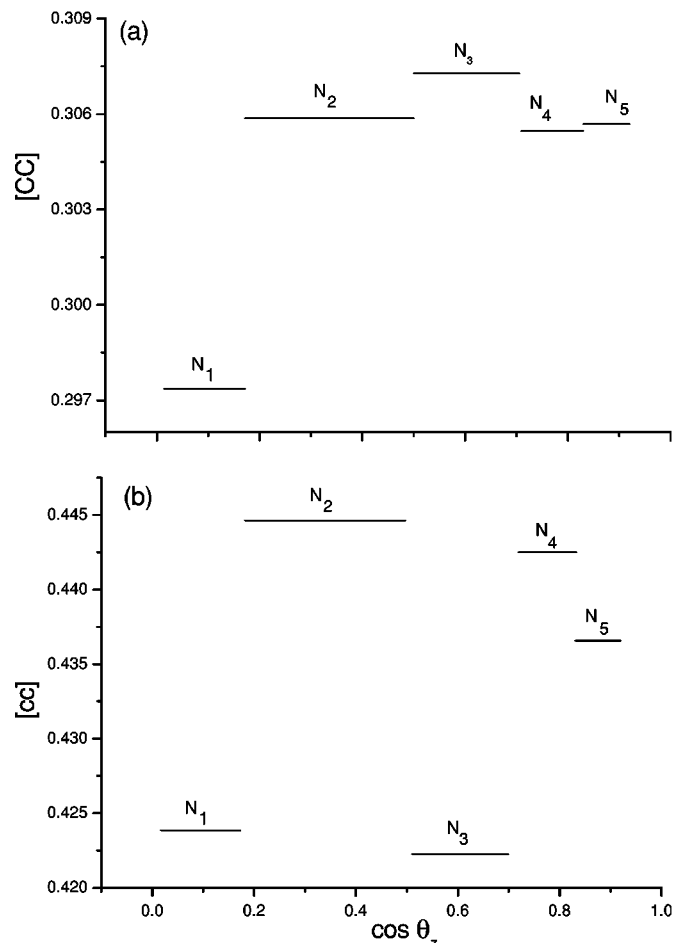

FIG. 3. Plot of the charged current event rates averaged over bins as a function of the zenith angles. (a) is for LMA which corresponds to the dashed line in Fig. 2; (b) is for the LOW corresponding to the dotted line in Fig. 2.

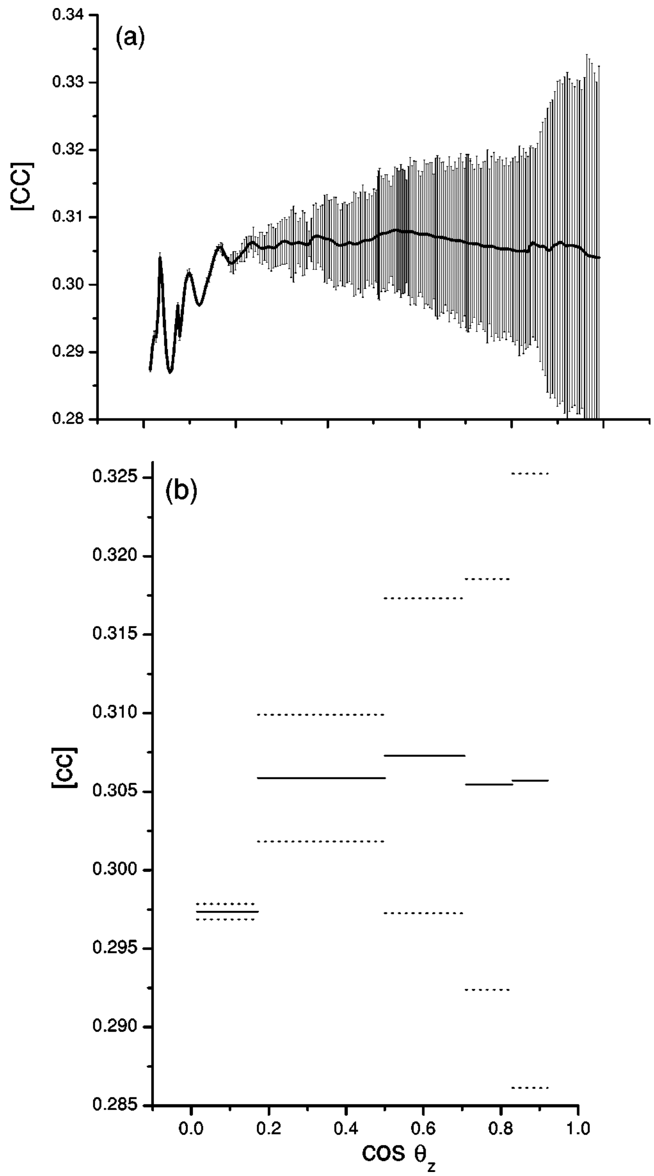

FIG. 4. Plot of the errors in the charged current event rates for the LMA vs the zenith angles. (a) shows the error bars attached on the dashed line of Fig. 2. (b) The solid line is the same as that in Fig. 3(a). Between the dotted lines are the errors caused by the uncertainty in the electron density.

defined to estimate the relevant error [14]. In this paper, however, we concentrate on the errors caused by the uncertainty of EED.

The EED available today is known only to some certain precision [15,16]. As to the PREM, significant uncertainties due to the local variation have been documented [17]. Quantitatively its precision is roughly 5% averaged per spherical shell with thickness of 100 km or so [18]. The uncertainties of Earth's matter density cause errors in the calculation of the ν_e survival probability during the nighttime. In the following we study numerically the uncertainties in the solar neutrino zenith angle distributions.

As described in detail in [7], we introduce a weighted average over the whole sample space of possible Earth's density profile. Denoting the averaged Earth's density function, such as the widely used PREM by $\hat{N}_e(x)$, we have $\hat{N}_e(x) = \langle N_e(x)\rangle = \int [DN_e] F[N_e(x),x][\mathcal{D}N_e]$, where $F[N_e(x),x]$ $[\mathcal{D}N_e]$ is the probability of obtaining the EED $N_e(x)$ in the neighborhood of x:

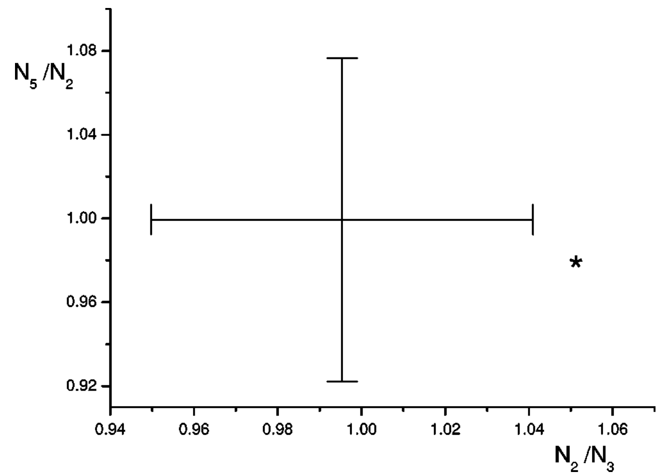

FIG. 5. Plot of the correlation between N_5/N_2 and N_2/N_3. The center of the cross corresponds to the best-fit LMA, the star is for the best-fit LOW. The error bars (cross) span a rectangle and indicate a possible blur due to the uncertainty of EED.

$$F[N_e(x),x] = \frac{1}{N_e(x)\sqrt{2\pi}s(x)} \times \exp\{-\ln^2[N_e(x)/N_0(x)]/[2s^2(x)]\},$$

$$s(x) = \sqrt{\ln[1+r^2(x)]},$$

$$N_0(x) = \hat{N}_e(x)\exp[-s^2(x)/2], \tag{9}$$

where $r(x) = \sigma(x)/\hat{N}_e(x)$ characterizes the precision of Earth's electron density.

The averaged value and the variance of the $\nu_2 \to \nu_e$ conversion probability can be written now separately as,

$$\langle P_{2e}(E_\nu,\theta_z)\rangle \equiv \int P_{2e}(\theta_z)F[N_e^{\theta_z}(x)][\mathcal{D}N_e^{\theta_z}]$$
$$= \lim_{I\to\infty}\int \prod_{i=1}^{I} F[N_e^{\theta_z}(x_i),x_i]dN_e^{\theta_z}(x_i)P_{2e}(\theta_z) \times [\{N_e^{\theta_z}(x_1),\ldots,N_e^{\theta_z}(x_i),\ldots,N_e^{\theta_z}(x_I)\}]$$
$$= \lim_{K\to\infty} K^{-1}\sum_{k=1}^{K} \tilde{P}_k(N_e^{(k)}),$$

$$\delta f_{reg} = \delta P_{2e}(E_\nu,\theta_z) \equiv \sqrt{\langle P_{2e}^2(E_\nu,\theta_z)\rangle - \langle P_{2e}(E_\nu,\theta_z)\rangle^2} = \left[\lim_{K\to\infty}(K-1)^{-1}\sum_{k=1}^{K}(\tilde{P}_k - \langle P_{2e}\rangle)^2\right]^{1/2}. \tag{10}$$

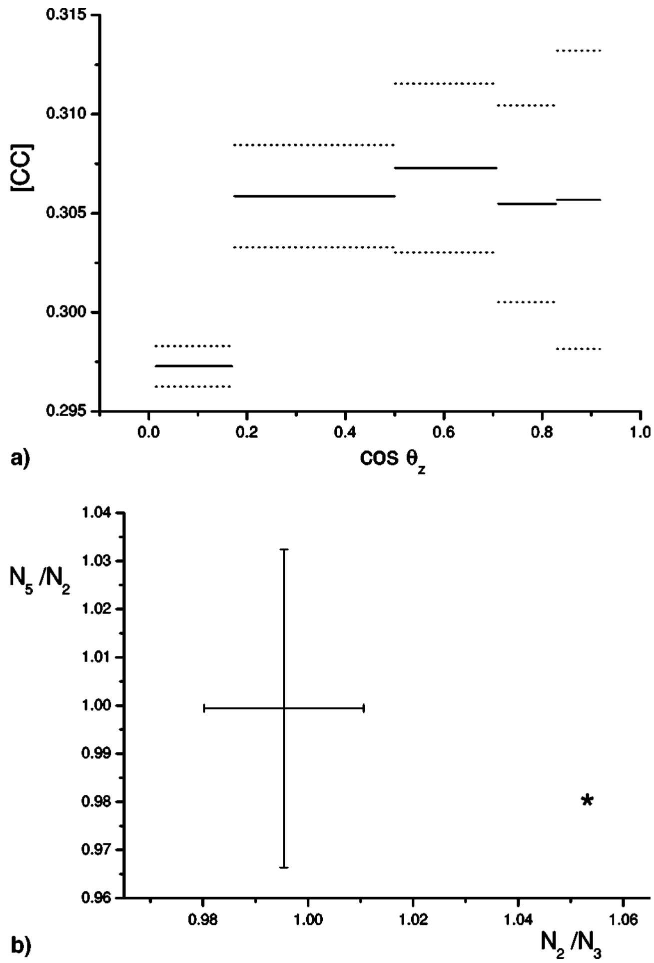

FIG. 6. (a) is the same as in Fig. 4(b), but with a 2% EED uncertainty in the AK135 model. (b) The same as Fig. 5, but with AK135 instead of the PREM.

We evaluate the functional integrations in Eq. (10) using a method similar to that of the lattice gauge theory. In the numerical calculation we discretize the neutrino path into I bins, δx_i $(i=1,2,\ldots,I)$ and in the ith bin the EED function $N_e(x)$ is given by Eq. (9). Furthermore, we have replaced the functional integration over the EED by a sum over K arrays, $N_e^{(k)} k=1,2,\ldots,K$. In Eq. (10) $\widetilde{P}_k$ is the conversion probability evaluated with the kth density profile $N_e^{(k)}$. As for the PREM each point in the array $N_e^{(k)}$ which consists of $N_e(x_1),\ldots,N_e(x_i),\ldots,N_e(x_I)$ is generated from the PREM weighted with a Gaussian-like logarithm distribution. Since the deviation from the PREM due to local variation is roughly 5% and the deviation is averaged per spherical shell with a thickness of 100 km, we take $r=5\%$ and choose the bin sizes δx_i to be the distance the neutrino travels along the path of the zenith angle θ_z within a spherical shell of thickness 100 km. So in general δx_i will not be equal except for $\theta_z=0$.

We note that the EED uncertainty scale δx differs from the one, $l_\rho=\rho/(d\rho/dx)$, considered in [6] to characterize the flatness (adiabaticity) of the density profile. Both of these scales are important to the studies on the neutrino oscillations in matter. The effects of the l_ρ can be taken into account in the exact numerical calculation; however, to reduce the error caused by δx a more precise density profile is needed. Especially when δx is comparable to the neutrino oscillation length in matter, one has to be careful in estimating the errors for oscillation probability.

In Fig. 1(b) we plot δf_{reg} and f_{reg} as a function of the zenith angle. One can see from this figure that the LMA suffers a larger error. For the LOW the error is roughly 2% and for the SMA the error is much smaller. So we have not shown them in the figure. Integrated over the zenith angle, it gives rise to a correction of 20% roughly to the A_{DN} for the LMA; however the corrections are small for the LOW and the SMA. Combined with Fig. 1(a), we see that the errors are small so that A_{DN}^{LMA} and A_{DN}^{LOW} can be distinguished.

To see the effects on the solar neutrino observations, we now estimate the errors in the rate of the charged current events during the night-time. Following [6] we define the normalized rate of the charged current events as

$$
\begin{aligned}
[CC](\theta_z) &\equiv N_{CC}/N_{CC}^{SSM}\\
&= \int_{E_{th}} dT_e \int_{E_\nu} dE_\nu P^N(E_\nu,\theta_z)\Phi(E_\nu)\\
&\quad \times \int dT' d\cos\theta_L \hat{\sigma}(E_\nu,T',\cos\theta_L)\\
&\quad \times R(T_e,T')/N_{CC}^{SSM}\\
&= \int_{E_\nu^0} dE_\nu \Phi(E_\nu) P^N(E_\nu,\theta_z)\sigma_{CC}(E_\nu)/N_{CC}^{SSM}, \quad (11)
\end{aligned}
$$

where $\Phi(E_\nu)$ contains both the neutrino flux from the boron decay and the He+P chain in the Sun [19,5], and N_{CC}^{SSM} is the normalization factor which equals the integral in the right-hand side taken at $P^N=1$. From the second to the third line of Eq. (11), the integration of the differential cross section $\hat{\sigma}$ with respect to the recoil electron kinetics T_e and the scatting angle θ_L has been replaced by a total charged current cross section σ_{CC} of the neutrino on the deuteron, since the possible uncertainty from T_e,θ_L can be canceled in the $[CC]$ as a ratio of N_{CC} to N_{CC}^{SSM}. The E_ν dependence in σ_{CC} is accessed by employing a *quick function* from *interpolation* in [20]. The starting point of the neutrino energy is set at $E_\nu^0 \approx Q+E_{th}$, with $Q=1.442$ MeV being the deuterium threshold energy and $E_{th}=5$ MeV the electron threshold energy. In Fig. 2 we plot the zenith angle distribution of the charged current events rate in Eq. (11). One can see that the SNO charged current data lies in the middle between the LMA and the LOW. This serves also as a check of our numerical calculation. Following the binning method of [6], we plot in Fig. 3(a) and Fig. 3(b) the charged current events vs bins [note for the fifth bin $\cos\theta_z \sim (0.83,0.92)$ in the case of the SNO], which shows that for the LMA

$$[N]_1<[N]_2\leqslant[N]_3\leqslant[N]_4\leqslant[N]_5, \quad (12a)$$

and for the LOW

$$[N]_2\geqslant[N]_4>[N]_1\sim[N]_3>[D]. \quad (12b)$$

Quantitatively, it reads, $[N]_5/[N]_2=0.999\approx 1$ and $[N]_2/[N]_3=0.995\approx 1$ for the LMA while $[N]_5/[N]_2=0.982, [N]_2/[N]_3=1.053$ for the LOW, from which it might be possible to distinguish the LMA from the LOW. The calculation for the SMA can be easily worked out; however, for simplicity we will not repeat it here.

Making use of Eqs. (3), (10), and (11) we estimate the errors in the charged current events rate caused by the uncertainties in Earth's electron density

$$\delta[CC]\propto\int_{E_\nu^0} dE_\nu \Phi(E_\nu)(-2X\delta f_{reg})\sigma_{CC}(E_\nu), \quad (13)$$

which we show in Fig. 4 by the error bars. To avoid multifold integration which is computer time consuming, we investigate δf_{reg} at neutrino energies of 8,10,11,12 MeV and find the results almost unchanged. To be conservative we have used the maximal value for δf_{reg}.

We see from the figure that the errors become larger as the zenith angle increases in the case of the LMA. Averaged over bins we have $([N]_5-\delta[N]_5)/[N]_2\approx 0.935$ while $([N]_2+\delta[N]_2)/([N]_3-\delta[N]_3)\approx 1.043$. As indicated in Figs. 13–16 of [6] that the LMA sheet in their correlation figures mainly stretched along the A_{DN} direction, we study a correlation between $[N]_5/[N]_2$ and $[N]_2/[N]_3$, which we show in Fig. 5. One sees that the point (1,1) for the LMA is swollen into a rectangle close to the point (0.982,1.053) for the LOW. In this figure we have not shown the error bars for the LOW since they are small.

So far we assume the precision of the PREM is 5%. Certainly errors on the zenith angle distribution become larger if the uncertainty in Earth's electron density is bigger. Sure a modern Earth's density model with higher precision will reduce the errors considered in this paper. As an example we take density model AK135 [21]. The precision of AK135 is widely considered to be about 1–2%, and its uncertainty scale is roughly $\delta x\approx 50$ km since the model was presented in a data table. Taking a 2% uncertainty in the electron density we show our results in Fig. 6. One finds $([N]_5-\delta[N]_5)/([N]_2+\delta[N]_2)\approx 1.033$ while $([N]_2+\delta[N]_2)/([N]_3-\delta[N]_3)\approx 1.017$. From Fig. 6(b), we see the gap between the LMA and the LOW enlarged. This makes it easier to distinguish the LMA from the LOW than the prediction from the PREM.

In summary, we have estimated in this paper the errors in the zenith angle distribution of the charged current event rates of the solar neutrinos originated from the electron density uncertainty. Our results show that the corrections are not significant in the cases of the LOW and the SMA; however, error is notable for the LMA. Even though our estimations are given for specific parameters and qualitatively, the results of this paper indicate that to observe the zenith angle distribution a precise knowledge of Earth's electron density is necessary.

The work is supported in part by the NSF of China under Grant No. 19925523 and also supported by the Ministry of Science and Technology of China under Grant No. NKBRSF G19990754.

[1] SNO Collaboration, Q. R. Ahmad *et al.*, Phys. Rev. Lett. **87**, 071301 (2001).

[2] Super-Kamiokande Collaboration, Y. Fukuda *et al.*, Phys. Rev. Lett. **82**, 1810 (1999).

[3] A. J. Baltz and J. Weneser, Phys. Rev. D **35**, 528 (1987); **37**, 3364 (1988); G. L. Fogli *et al.*, IASSNS-AST 96/21; J. N. Bahcall, P. I. Krastev, and A. Yu. Smirnov, Phys. Rev. D **60**, 093001 (1999).

[4] E. Lisi and D. Montanio, Phys. Rev. D **56**, 1792 (1997).

[5] G. L. Fogli *et al.*, Phys. Rev. D **62**, 113003 (2000); V. Barger *et al.*, *ibid.* **64**, 073009 (2001).

[6] M. C. Gonzalez-Garcia *et al.*, Phys. Rev. D **63**, 113004 (2001).

[7] Lian-You Shan, Bing-Lin Young, and Xinmin Zhang, hep-ph/0110414.

[8] A. S. Dighe, Q. Y. Liu, and A. Yu. Smirnov, hep-ph/9903329.

[9] S. T. Petcov, Theory of Neutino Oscillations, 6th School on Non-accelerator Astroparticle Physics, ICTP, Trieste, 2001.

[10] A. M. Dziewonsky and D. L. Andson, Phys. Earth Planet. Inter. **25**, 297 (1981).

[11] D. Marfatia, V. Barger, and K. Whisnant, Phys. Rev. Lett. **88**, 011302 (2002); P. I. Krastev and A. Yu. Smirnov, Phys. Rev. D **65**, 073022 (2002); J. N. Bachall *et al.*, J. High Energy Phys. **04**, 007 (2002).

[12] Electron density distribution is available at the website of J. N. Bahcall.

[13] F. N. Loreti and A. B. Balantekin, Phys. Rev. D **50**, 4762 (1994); H. Nunokawa *et al.*, Nucl. Phys. **B472**, 495 (1996); C. P. Burgess and D. Michaud, Ann. Phys. (N.Y.) **256**, 1 (1997).

[14] A. B. Balantekin, J. M. Fetter, and F. N. Loreti, Phys. Rev. D **54**, 3941 (1996).

[15] B. Jacobsson *et al.*, Phys. Lett. B **532**, 259 (2002).

[16] R. J. Geller and T. Hara, hep-ph/0111342.

[17] R. Jeanlow and S. Morris, Annu. Rev. Earth Planet Sci. **14**, 377 (1986); R. Jeanlow, *ibid.* **18**, 357 (1990); Fu-Tian Liu *et al.*, Geophys. J. Int. **101**, 379 (1990); T. P. Yegorova *et al.*, *ibid.* **132**, 283 (1998); B. Romanowicz, Geophys. Res. Lett. **28**, 1107 (2001).

[18] B. A. Bolt, Q. J. R. Astron. Soc. **32**, 367 (1991).

[19] J. N. Bahcall *et al.*, Phys. Rev. C **54**, 411 (1996); J. N. Bahcall, *ibid.* **56**, 3391 (1997).

[20] J. N. Bahcall and E. Lisi, Phys. Rev. D **54**, 5417 (1996).

[21] B. L. N. Kennett *et al.*, Geophys. J. Int. **122**, 108 (1995); J. P. Montagner *et al.*, *ibid.* **125**, 229 (1995).